Hindawi
Journal of Electrical and Computer Engineering
Volume 2017, Article ID 7948571, 6 pages
https://doi.org/10.1155/2017/7948571

Research Article

The 2D Spectral Intrinsic Decomposition Method Applied to Image Analysis

Samba Sidibe, Oumar Niang, Abdoulaye Thioune, Abdoul-Dalibou Abdou, and Ndeye Fatou Ngom

Laboratoire de Traitement de l'Information et Systèmes Intelligents, Ecole Polytechnique de Thiès, BP A10, Thiès, Senegal

Correspondence should be addressed to Oumar Niang; oniang@ucad.sn

Received 5 July 2016; Revised 4 January 2017; Accepted 18 January 2017; Published 20 December 2017

Academic Editor: M. Jamal Deen

We propose a new method for autoadaptive image decomposition and recomposition based on the two-dimensional version of the Spectral Intrinsic Decomposition (SID). We introduce a faster diffusivity function for the computation of the mean envelope operator which provides the components of the SID algorithm for any signal. The 2D version of SID algorithm is implemented and applied to some very known images test. We extracted relevant components and obtained promising results in images analysis applications.

1. Introduction

The need of components extraction and reconstruction in signal and image processing in time frequency analysis is very strong for many fields of application. Notorious methods that have been proposed include Fourier technics, wavelet decomposition, and Empirical Mode Decomposition. While Fourier transform is localized in frequency, wavelets are localized in both time and frequency; EMD is autoadaptive. EMD decomposes a signal in AM-FM components called Intrinsic Mode Functions (IMF) and a residue. This nonlinear and nonstationary decomposition works on 1D signals [1] and 2D signals such as images [2, 3]. The EMD algorithm is based on a procedure called sifting process which iteratively uses the upper and lower envelopes to extract IMFs. To create a mathematical model to compute envelopes directly, an envelope operator has been proposed in [4] and from this operator a new decomposition method called Spectral Intrinsic Decomposition, SID, was proposed in [5].

The SID method allows decomposing any signal into a superposition of Spectral Proper Mode Functions (SPMFs) [5]. This method has been presented in a 1D version and depends on an operator interpolating the characteristics points of the signal to be decomposed. In this paper, the two-dimensional version of the Spectral Intrinsic Decomposition for images analysis is introduced. An algorithm for a faster spectral decomposition is proposed and illustrated with some images. We first recall the SID principle in one dimension and propose a faster method to determine the signal characteristics points in Section 2. Than an algorithm of the two-dimensional SID is presented in Section 3. Applications on grayscale images are depicted in Section 3.1.

2. The Spectral Intrinsic Decomposition Method

The Spectral Intrinsic Decomposition Method decomposes any signal into a combination of eigenvectors of a Partial Differential Equation (PDE) interpolation operator as presented in [5, 6].

2.1. The PDEs System Interpolator. For a given signal s_0, the upper (s^+) and lower (s^-) envelope are the asymptotic solution of the following PDEs system:

$$\frac{\partial s^{\pm}(x,t)}{\partial t} = -g^{\pm}(x,t)\left(\alpha\frac{\partial^2 s^{\pm}(x,t)}{\partial^2 x} + (1-\alpha)\frac{\partial^4 s^{\pm}(x,t)}{\partial^4 x}\right), \quad (1)$$

$$s^{\pm}(x,0) = s_0.$$

α is the tension parameter which ranges from 0 to 1. g^+ and g^- are diffusivity functions for upper and lower envelope which are equal to zero at characteristic points of s_0 and range from zero to one. $g^\pm$ based on Maximum Curvature Points (MCP) can be computed as follows:

$$g^{\pm}(x) = \frac{1}{9}\left[\left|\operatorname{sgn}\left(\frac{\partial^3 s_0(x)}{\partial^3 x}\right)\right| \pm \operatorname{sgn}\left(\frac{\partial^2 s_0(x)}{\partial^2 x}\right) + 1\right]^2, \quad (2)$$

where sgn denotes the sign function.

Equation (1) is resolved numerically in its discrete implicit unconditionally stable scheme as follows:

$$S^{k+1} = S^k + \Delta t A S^{k+1}, \quad S^0 = S_0, \quad (3)$$

where Δt is the time step, $S^{k+1} = s(x, k\Delta t)$ is signal value at step $k+1$, and A is a matrix formed with finite difference approximation coefficients of second- and fourth-order differential operators (resp., D_2 and D_4), as $A = G(\alpha D_2 - (1-\alpha)D_4)$, with G being the diagonal matrix constructed with discrete version of stopping function values $g(x)$, exactly, $G(i,i) = g(i)$.

So the explicit form leads to the following numerical resolution:

$$S^{k+1} = (I - \Delta t A)^{-1} S^k, \quad S^0 = s_0, \ k \geq 0 \quad (4)$$

with I being the identity matrix. Finally (1) can be decomposed into a linear system from implicit numerical scheme (4) by

$$S^{(k+1)} = L^{-1} S^k, \quad S^0 = s_0, \ k \geq 0. \quad (5)$$

L is given by $L = I - \Delta t A$.

The operator matrix, L, has real-valued eigenvalues that are always greater than or equal to 1. Then, eigenvalues, λ_n, of L^{-1} are always smaller than or equal to 1 ($0 < \lambda_n \leq 1$); see [4].

2.2. On the Asymptotic Solution. Iterative scheme (5) can be rewritten in terms of initial solution s_0 as

$$S^k = \left(L^{-1}\right)^k s_0, \quad k \geq 1. \quad (6)$$

After convergence (see [7]), the asymptotic solution, S^∞, is given by

$$S^\infty = \left(L^{-1}\right)^\infty s_0. \quad (7)$$

Let V be a matrix of L^{-1}'s sequence of eigenvectors (V_n) and $\mathcal{D}$ a diagonal matrix having L^{-1}'s sequence of eigenvalues (λ_n), at the diagonal. So we have the following decomposition $L^{-1} = V\mathcal{D}V^{-1}$. It is easy to see that

$$\left(L^{-1}\right)^k = \left(V\mathcal{D}V^{-1}\right)^k = VD^kV^{-1}. \quad (8)$$

So, the asymptotic solution in (7) is given by

$$S^\infty = \left(V\mathcal{D}^\infty V^{-1}\right) S_0. \quad (9)$$

The asymptotic eigenvalue matrix $\mathcal{D}^\infty$ is a diagonal matrix with eigenvalues $\lambda_n^\infty = 1$ only at loci where matrix G is zeroed, and $\lambda_n^\infty = 0$, where $g[n] > 0$. Finally, the asymptotic solution of the PDE interpolator system is a linear combination of fixed vector point of upper and lower envelope operators.

2.3. A Faster Stopping Function for Discrete Signal. For image processing we will consider region boundaries as characteristic points. The characteristic points of the upper envelope will be the local maximums and the limits of the regions where the value of the gray level of the pixel is equal to or greater than the gray level of all the pixels in their neighborhood represented, for example, by a rectangular window.

We define the diffusion function g_M^- for lower envelope to be equal to 1 everywhere except in characteristic points of the lower envelope where it will be equal to 0.

Similarly the characteristic points of the lower envelope are local minimums and region boundaries where the pixel value is equal to or less than the gray level of all pixels in their neighbors. We define the diffusion function g_M^+ for upper envelope to be equal to 1 everywhere except in characteristics points of the upper envelope where it will be equal to 0.

The diffusivity function called stopping function $g_M^\pm$ is calculated by using morphological dilation and erosion operations [8].

Let $b = [-1, 0, 1]$ be a structured element; the grayscale dilation of s by b at x is given by

$$[s \oplus b](x) = \max_{a \in b} \{s(x+a)\}. \quad (10)$$

The grayscale erosion of s by b at x is given by

$$[s \ominus b](x) = \min_{a \in b} \{s(x+a)\}. \quad (11)$$

$s \oplus b$ is equal to s at local maxima and when s is locally constant; $s \ominus b$ is equal to s at local minima and when s is locally constant.

g_M^+ is zeroed at points which are invariant to morphological dilation and variant to morphological erosion; g_M^+ is equal to 1 for any other point.

Similarly, g_M^- is zeroed at points which are invariant to morphological erosion and variant to morphological dilation; g_M^- is equal to 1 for any other point.

Let

$$A = \{x \mid [s \oplus b](x) = s(x)\}, \quad B = \{x \mid [s \ominus b](x) = s(x)\}. \quad (12)$$

We have

$$g_M^+(x) = \begin{cases} 0, & \text{if } x \in A \setminus B, \\ 1, & \text{otherwise}, \end{cases} \quad g_M^-(x) = \begin{cases} 0, & \text{if } x \in B \setminus A, \\ 1, & \text{otherwise} \end{cases} \quad (13)$$

Table 1

Image	Width	Height	Time for $g^{\pm}$	Time for $g_M^{\pm}$
Figure 4(a)	300	300	0,4684466	0.320695
Figure 3(a)	400	266	0,826974833	0,2877035
Figure 2(a)	400	272	0,807968	0,284108

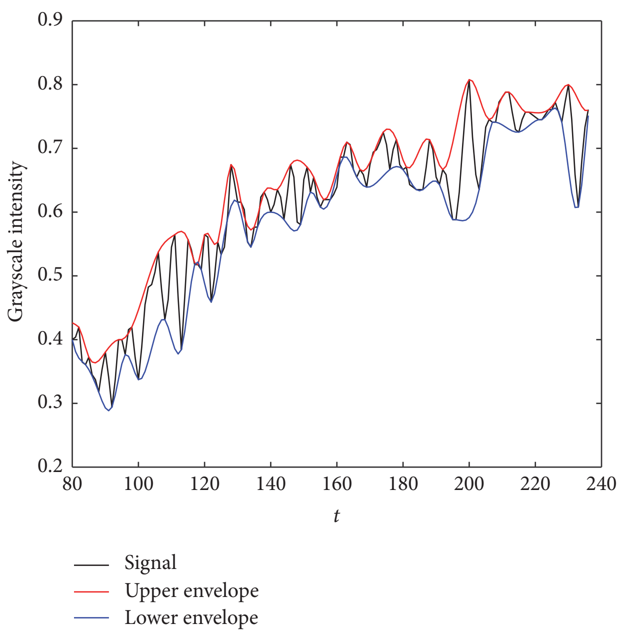

Figure 1: The effectiveness of envelope computation using g_M instead of g.

g_M functions are faster than g to compute and give satisfying results for the computation of envelope operators for real images (Table 1).

Figure 1 shows an example of calculating the envelope using g_M, g_M^+ for upper envelope and g_M^- for lower envelope.

2.4. The Spectral Intrinsic Decomposition. In the following, E denotes either the upper or lower envelope operator. The upper and lower envelope of the signal are calculated with the eigenvectors associated with eigenvalue $\lambda = 1$. Hence, S^{∞} in formula (9) is a linear combination of all 1-eigenvectors of the envelope operator E weighted by the signal amplitude. Instead of focusing only on the envelope calculus, we now consider all the set of eigenvalues of the envelope operator E.

The Spectral Intrinsic Decomposition procedure is defined as the calculus of all the SPMFs for a given signal. $E = L^{-1}$. The same procedure can be performed with the lower envelope. The eigendecomposition of E gives $[V_E, L_E] = \text{eig}(E)$, where $V_E = [V_1, \ldots, V_{\text{size}(s0)}]$ and $L_E = [L_1, \ldots, L_{\text{size}(s0)}]$ (with the possibility of zeros to complete the size of the vector) are, respectively, the set of eigenvectors and the set of eigenvalues of E. The coefficient reconstruction of s_0 is given by $C = L_E V_E^{-1} s_0^{\perp}$, with $s_0^{\perp}$ being the transpose of s_0.

(1) $M \leftarrow$ transforme image to data
(2) NL $\leftarrow$ number of lines of M
(3) NC $\leftarrow$ number of columns of M
(4) $M_R \leftarrow$ NL by NC zeroed matrix
(5) **for** $i \leftarrow 1$, NL **do**
(6) $s_i \leftarrow$ line i of M
(7) compute g_i^+ from s_i
(8) compute E_i
(9) decompose E_i, $[V_{E_i}, L_{E_i}] \leftarrow \text{eig}(E)$
(10) compute C_i, $C_i = L_{E_i} V_{E_i}^{-1} s_i'$
(11) **for** $j \leftarrow 1$, NC **do**
(12) $M_R(i, j) \leftarrow V_i(j) * C_i(j)$
(13) **end for**
(14) **end for**
(15) recompose image from M_R

Algorithm 1: Pseudocode for decomposition and recomposition.

Hence s_0 is computed by the formula $s0 = VC$ (Algorithm 2). The Spectral Intrinsic Decomposition of s_0 is given as follows:

$$s_0 = \sum_{k=1}^{N} V_k C_k, \quad N = \text{size}(s_0). \tag{14}$$

This decomposition is intrinsic and depends only on the position of the characteristic points of s_0 that define the diffusivity function in the interpolation operator. We notice that the SID with lower envelope works like the SID with the upper envelope and has the same reconstruction ability.

2.5. Advantage and Disadvantage of SID. The SID is adaptive and depends on the position of the characteristics points of the signal. It is autoadaptive and works for nonlinear and nonstationary signal. SID can decompose an IMF and can be used to separate mixing mode [9] in EMD.

However, the main disadvantage of the proposed SID algorithm is the computation time when the size of signal is a large. This is due to matrix inversion in the algorithm. Thus a faster algorithm is proposed in the next section.

3. The 2D Spectral Intrinsic Decomposition Algorithm

In this section we present, in Algorithm 1, the 2D SID procedure and implement it for images decomposition-recomposition.

3.1. The Algorithm of Image Decomposition and Recomposition by SID. Let us consider an image as represented by a matrix M *(Line (1))*. Each row i of the matrix M *(Line (5))* can be seen as a one-dimensional signal s_i. Thus, we can apply the spectral decomposition of s_i *(Lines (6) to (10))* as described in [4].

Each line can be recomposed to build a matrix M_R *(Lines (11) to (13))* and finally reconstruct the image from M_R *(Line (15))*. Image decomposition and recomposition are described in Algorithm 1. We can also make decomposition

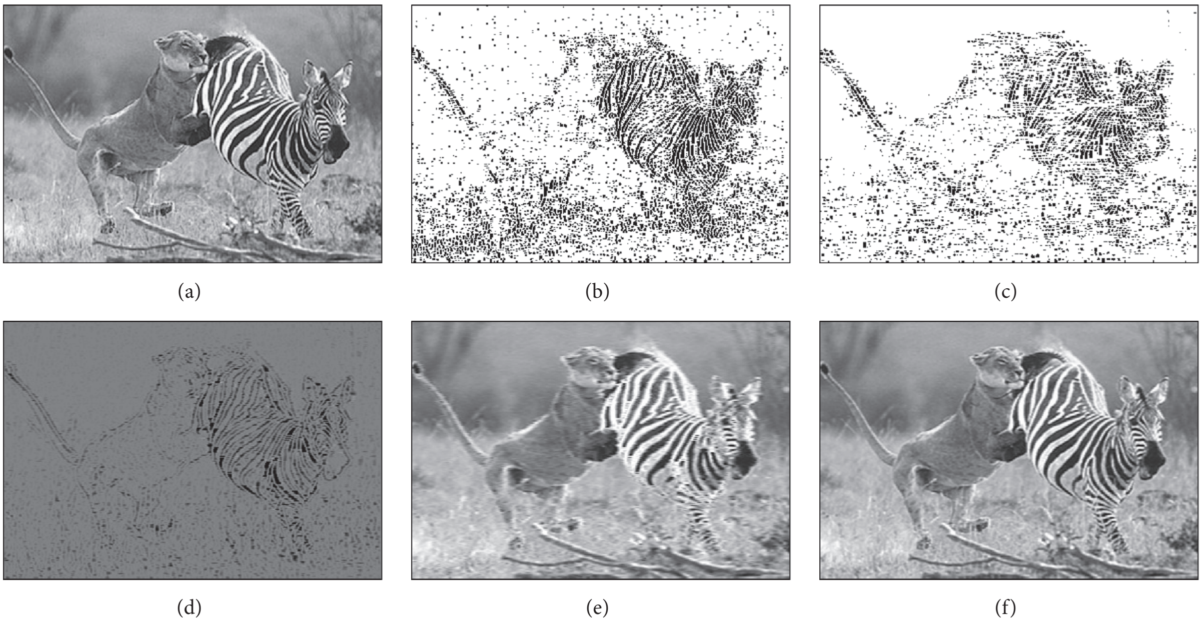

Figure 2: Decomposition (a), component extraction and representation of high frequency component ($\lambda \in [0, 0.1]$) (b), medium frequency component ($\lambda \in [0.5, 0.7]$) (c), high and medium frequency component ($\lambda < 1$) (d), low frequency component ($\lambda = 1$) (e), and recomposition of all components (f).

$[\lambda_{\min}, \lambda_{\max}] \leftarrow$ eigenvalues interval to extract
$M \leftarrow$ transforms image to data
NL $\leftarrow$ number of lines of M
NC $\leftarrow$ number of columns of M
$M_R \leftarrow$ NL by NC zeroed matrix
for $i \leftarrow 1$, NL **do**
    $S_i \leftarrow$ line i of M
    compute g_i^+ from s_i
    compute E_i
    decompose E_i, $[V_{E_i}, L_{E_i}] \leftarrow \mathrm{eig}(E)$
    $L_{R_i} \leftarrow L_{E_i}$
    for $j \leftarrow 1$, NC **do**
        if $L_{R_i}(j) \le \lambda_{\min}$ or $L_{R_i}(j) \ge \lambda_{\max}$ **then**
            $L_{R_i}(j) \leftarrow 0$
        end if
    end for
    compute C_{R_i}, $C_{R_i} \leftarrow L_{R_i} V_{E_i}^{-1} S_i'$
    for $j \leftarrow 1$, NC **do**
        $M_R(i, j) \leftarrow M_R(i, j) + V_{E_i}(j) * C_{R_i}(j)$
    end for
end for

Algorithm 2: Pseudocode to extract SPMFs between two eigenvalues.

along columns and catch more properties of the image to be analyzed.

The elementary components of a spectral decomposition are the modulation of eigenvectors by their coefficients as can be seen in (14). It is clear that these components depend on eigenvalues of the envelope operator.

The range of smallest eigenvalues catches higher frequencies contents of the reconstructed signal with the smallest modulated amplitude.

So we can associate components which have similar frequency and amplitude by summing the components that have same eigenvalues; this method works well for signal in one dimension. For images, it is possible numerically to have missing eigenvalues in many lines. Hence, to avoid this drawback, elementary components which have the same eigenvalues will be associated with the same belonging to a specific range of eigenvalues.

3.2. Application to Image Components Extraction. In the following, 2D SID is applied to very known images test to demonstrate the ability of this pectoral intrinsic decomposition for images analysis, particularly in components extraction. In Figures 4(a), 3(a), and 2(a), we have a representation of high frequency components on Figures 4(b), 3(b), and 2(b); we note that they are more sensitive to small variations of the intensity of the image than low frequencies components in Figures 4(c), 3(c), and 2(c).

4. Conclusion

In this paper, we have presented a new method for autoadaptive image representation called two-dimensional version of the Spectral Intrinsic Decomposition. A new faster diffusivity function in the computation of the mean envelope operator is also provided. In future works, we will investigate how to use the Spectral Proper Mode Functions (SPMFs) to do signals classification or to treat other aspects of image processing, like edge detection, segmentation, and so on.

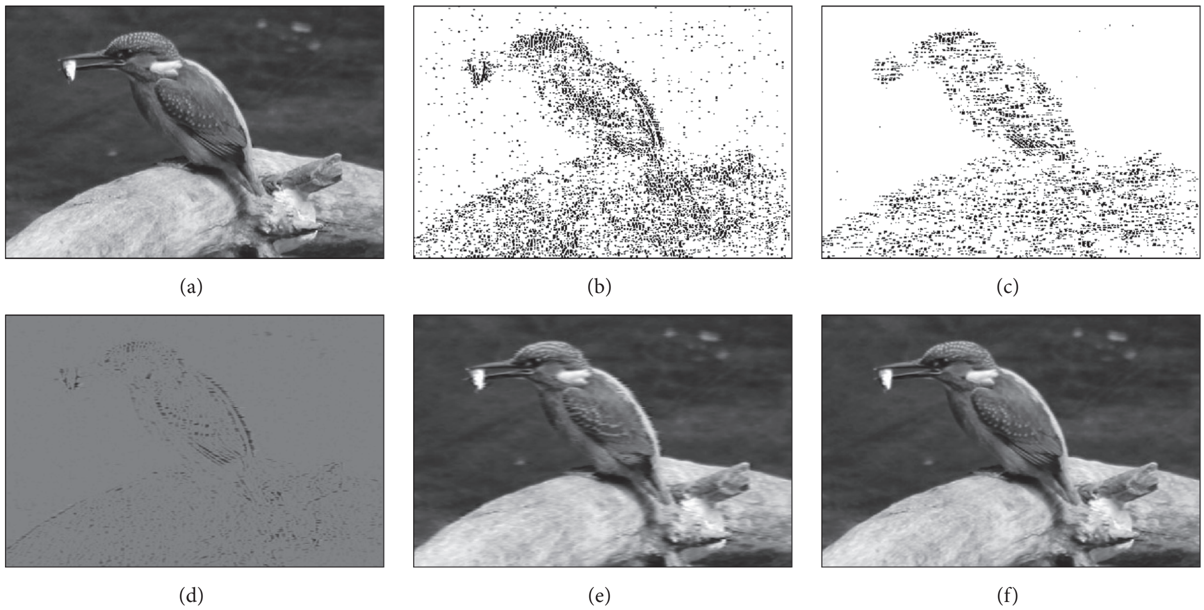

Figure 3: Decomposition (a), component extraction and representation of high frequency component ($\lambda \in [0, 0.1]$) (b), medium frequency component ($\lambda \in [0.5, 0.7]$) (c), high and medium frequency component ($\lambda < 1$) (d), low frequency component ($\lambda = 1$) (e), and recomposition of all components (f).

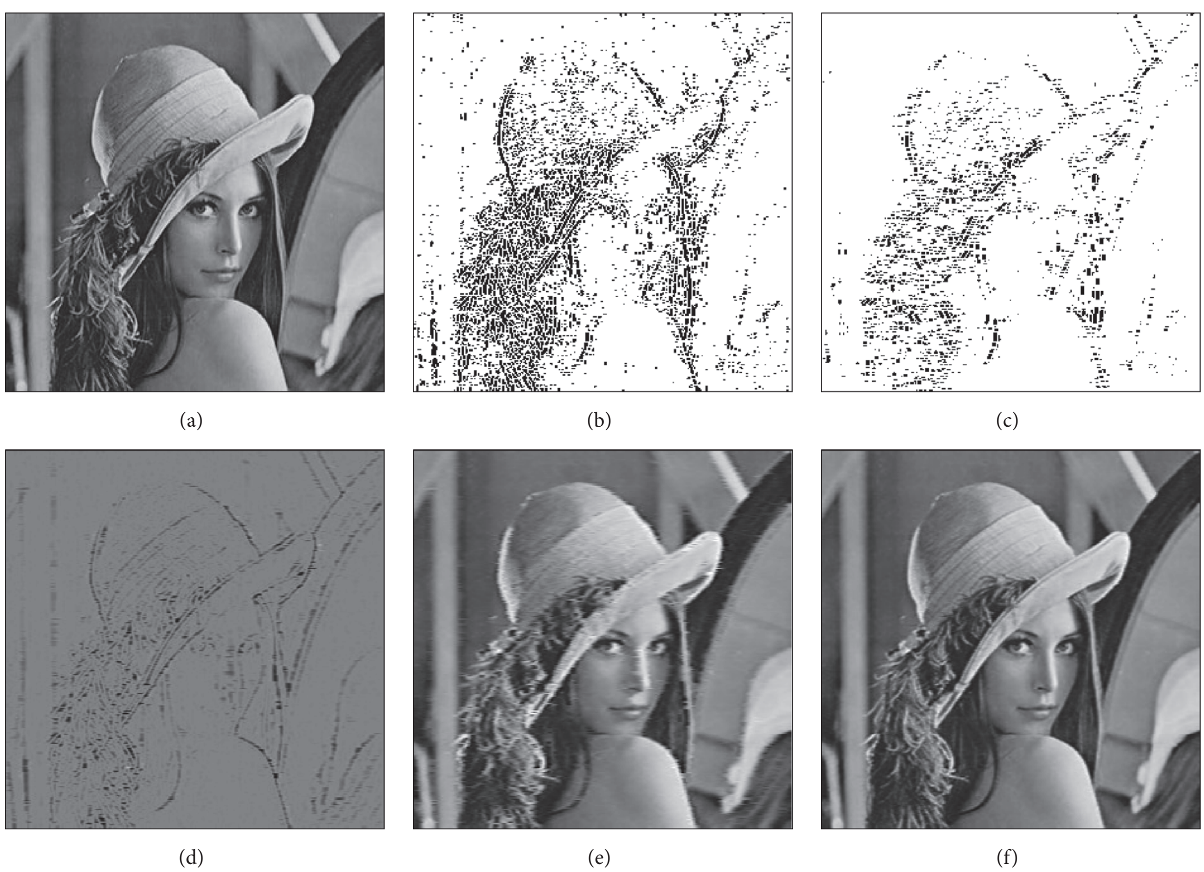

Figure 4: Decomposition (a), component extraction and representation of high frequency component ($\lambda \in [0, 0.1]$) (b), medium frequency component ($\lambda \in [0.5, 0.7]$) (c), high and medium frequency component ($\lambda < 1$) (d), low frequency component ($\lambda = 1$) (e), and recomposition of all components (f).

Conflicts of Interest

The authors declare that they have no conflicts of interest.

References

[1] N. E. Huang, Z. Shen, S. R. Long et al., “The empirical mode decomposition and the Hilbert spectrum for nonlinear and non-stationary time series analysis,” *Proceedings A*, vol. 454, no. 1971, pp. 903–995, 1998.

[2] J. C. Nunes, Y. Bouaoune, E. Delechelle, O. Niang, and P. Bunel, “Image analysis by bidimensional empirical mode decomposition,” *Image and Vision Computing*, vol. 21, no. 12, pp. 1019–1026, 2003.

[3] F. B. Arfia, A. Sabri, M. B. Messaoud, and M. Abid, “The Modified Bidimensional Empirical Mode Decomposition for Color Image Decomposition,” in *Proceedings of the World Congress on Engineering*, vol. 2, 2011.

[4] O. Niang, É. Deléchelle, and J. Lemoine, “A spectral approach for sifting process in empirical mode decomposition,” *Signal Processing, IEEE Transactions on*, vol. 58, no. 11, pp. 5612–5623, 2010.

[5] O. Niang, A. Thioune, É. Deléchelle, and J. Lemoine, “Spectral Intrinsic Decomposition Method for Adaptive Signal Representation,” *ISRN Signal Processing*, vol. 2012, pp. 1–10, 2012.

[6] O. Niang, *Décomposition Modale Empirique: Contribution à la Modélisation Mathématique et Application en Traitement du Signal et de lImage [Ph.D. thesis]*, Université Paris XII Val de Marne, 2007.

[7] O. Niang, A. Thioune, É. Deléchelle, M. T. Niane, and J. Lemoine, “About a Partial Differential Equation-Based Interpolator for Signal Envelope Computing: Existence Results and Applications,” *ISRN Signal Processing*, vol. 2013, pp. 1–18, 2013.

[8] L. Vincent, “Morphological grayscale reconstruction in image analysis: applications and efficient algorithms,” *IEEE Transactions on Image Processing*, vol. 2, no. 2, pp. 176–201, 1993.

[9] Y. Gao, G. Ge, Z. Sheng, and E. Sang, “Analysis and solution to the mode mixing phenomenon in EMD,” in *Proceedings of the 1st International Congress on Image and Signal Processing, CISP 2008*, pp. 223–227, May 2008.